Research Paper
Computational Methods for Differential Equations
http://cmde.tabrizu.ac.ir
Vol. *, No. *, *, pp. 1-20
DOI:10.22034/cmde.2025.66680.3142

A study of weighted b-spline method for solving nonlocal subdiffusion model

Jitesh P. Mandaliya[1,*] **and Dileep Kumar**[2]

[1]Department of Mathematics, Institute of Infrastructure, Technology, Research and Management, Ahmedabad, Gujarat, India.

[2]Department of Mathematics, Government Post Graduate College Noida, Uttar Pradesh, India.

Abstract

In this study, we employ weighted b-splines to obtain the numerical solution for the nonlocal subdiffusion equation widely used in population dynamics. For spatial discretization, we utilize weighted b-spline method that is computationally efficient, providing accurate results with fewer parameters. The temporal discretization is performed using $L1$ and $L2\text{-}1_\sigma$ schemes on a graded mesh. We establish the existence, uniqueness, and regularity of the solution at the continuous level. Furthermore, we derive *a priori* error bounds and convergence estimates in both $L^2(\Omega)$ and $H_0^1(\Omega)$ norms using a α-robust discrete Gronwall inequality. The theoretical findings are validated through three numerical examples.

Keywords. Mesh-free method, Weighted b-spline, $L1$ and $L2\text{-}1_\sigma$ methods.

2010 Mathematics Subject Classification. 74S05, 65L70, 65D07.

1. Introduction

The present research work focuses on solving the following nonlocal subdiffusion equation:

$$ {}_0^cD_t^\alpha u - M\left(\int_\Omega u\,dx\right)\Delta u = f(x,t) \quad \text{in} \quad \Sigma, \tag{1.1a} $$

$$ u(x,t) = 0 \quad \text{on} \quad \partial\Sigma, \tag{1.1b} $$

$$ u(x,0) = u_0(x) \quad \text{in} \quad \Omega \tag{1.1c} $$

where $\Omega \subseteq \mathbb{R}^2$ is a bounded domain with sufficiently smooth boundary $\partial\Omega$, and $\Sigma = \Omega \times (0,T]$, $\partial\Sigma = \partial\Omega \times (0,T]$. The term ${}_0^cD_t^\alpha u(x,t)$ is the α^{th}-order Caputo fractional derivative of u with $\alpha \in (0,1]$, and it is defined [9] as

$$ {}_0^cD_t^\alpha u(x,t) := \begin{cases} \frac{1}{\Gamma(1-\alpha)} \int_0^t (t-s)^{-\alpha}\, \frac{\partial u(x,s)}{\partial s}\, ds & \text{for} \quad 0<\alpha<1, \\ \frac{du(x,t)}{dt} & \text{for} \quad \alpha = 1. \end{cases} $$

The nonlocal diffusion term frequently arises in the modeling of various physical and biological phenomena. For instance, while modeling the dynamics of bacterial population through (1.1a), u represents the density of the bacterial population, and the nonlocal term M is the diffusion coefficient that depends on the characteristic of density of the population across the entire domain [4, 8]. Fractional-order differential equations naturally connect to memory-related models, particularly those describing anomalous diffusion phenomena frequently observed in various scientific fields, such as the diffusion of pollutants in the atmosphere, fluctuations in stock prices, and the movement of proteins within cells [21, 25].

Since analytical solutions for time-fractional PDEs are known only for special cases, some efficient numerical techniques are required to solve such problems. Several research articles propose various numerical methods to solve time-fractional differential equations. The $L1$ method [2, 6, 9, 28, 30] and the $L2\text{-}1_\sigma$

Received: 08 April 2025 ; Accepted: 08 August 2025.
∗ Corresponding author. Email: jitesh.mandaliya.20pm@iitram.ac.in.

method also known as the fractional Crank-Nicolson method [1, 7, 16, 29], have been widely used for temporal discretization and finite element method (FEM) [17, 18, 22], finite difference method [30], mixed FEM [15], etc., are commonly used for spatial discretization. Among these methods, the FEM has been explored significantly for solving a variety of fractional PDEs.

The authors in [18] considered a nonlinear time-fractional diffusion equation in terms of the Caputo fractional derivative of order $\alpha \in (0,1)$. They discussed the well-posedness as well as the regularity of the solution by employing the Lipschitz continuity of the nonlinear source term. In the case of weak singularity at time $t = 0$ for the solution of a subdiffusion equation, the $L1$ method-based scheme on a uniform grid provides only $O(\tau^{\alpha})$ convergence order in the maximum norm (cf. [18]), where τ denotes the time step size. M. Stynes et al. [30] considered a linear subdiffusion equation and solved it by taking the weak singularity into account at initial time $t = 0$. They analyzed the problem using the $L1$-finite difference method on a graded mesh and provided sharp convergence results for the numerical solution in the $L^{\infty}(\Omega)$ norm. In [27], the authors utilized a cubic spline difference scheme for spatial discretization and the $L1$ scheme on a graded mesh for temporal discretization to obtain a robust fully-discrete scheme for solving the time-fractional reaction-diffusion equations. Furthermore, the standard finite element technique on a quasi-uniform mesh in the spatial direction and the $L1$ method on a suitably graded mesh in the temporal direction is employed in [5] to achieve the optimal convergence of $O(\tau^{2-\alpha})$ in the temporal direction. Additionally, in [5], the authors derived α-nonrobust error estimate for problem (1.1). Unlike [5], in this paper, we derive α-robust error estimate for the problem (1.1).

$L1$ based scheme for fractional differential equation results in convergence $O(\tau^{2-\alpha})$ clearly signifying an inverse relation with α i.e., larger(smaller) α values give slower(faster) convergence rate. To overcome this limitation and to obtain optimal order in the temporal direction, Alikhanov [1] introduced a new scheme on a uniform mesh called the $L2\text{-}1_{\sigma}$ scheme for finding the numerical solution of the linear time-fractional diffusion equation. The scheme attains $O(\tau^2)$ convergence order, thereby making it independent of fractional derivative order α. But in case of a weak singularity of the solution, both methods can attain only $O(\tau^{\alpha})$ convergence order. Thus, similar to the $L1$ method, $L2\text{-}1_{\sigma}$ method is also explored for graded/general non-uniform meshes in many works (see [7, 16, 17, 33] and references therein).

Description of the geometry of the domain and generating mesh are often challenging and time-consuming in the FEM. To overcome this issue, Höllig et al. [12] proposed a new method known as the weighted extended b-spline (web-spline) method, which is a mesh-free method since it does not require any mesh generation. This method is developed within the framework of the standard FEM. It introduces a new finite element subspace containing web-splines as the basis functions. In the following, we mention some advantages of the web-spline method, which include [12, 13]:

- Method requires no mesh generation.
- Dirichlet boundary conditions are represented exactly.
- Accurate approximations can be achieved using relatively few parameters.
- An Arbitrary approximation order can be chosen.

Numerous studies in the existing literature explore the use of the spline based method to obtain numerical solutions for classical elliptic [12] and parabolic [3, 11, 20, 23, 24, 29] PDEs. In [3], the authors studied parabolic nonlocal initial boundary value problems, deriving web-spline based error estimates in $L^2(\Omega)$ and $H_0^1(\Omega)$ norms. In [24], the authors considered the heat equation with Dirichlet boundary conditions and solved numerically using web-splines of degree m ($m = 1, 2, 3$). Additionally, the authors in [11] utilized cubic trigonometric b-splines and non-polynomial spline methods to solve nonlinear coupled time-fractional Schrödinger equations. In [23], the authors proposed a mesh-free method based on radial basis functions to solve 2D fractional PDEs on irregular domains. Furthermore, the authors in [20] applied a linear b-splines for spatial discretization and the Crank-Nicolson scheme for temporal discretization to solve the delay reaction-diffusion equation.

Motivated by the above literature, we propose a scheme involving weighted b-spline with $L1$ and $L2\text{-}1_{\sigma}$ methods on graded grids to solve the time-fractional nonlocal diffusion problem (1.1).

The main contributions of the proposed work are summarized as follows:

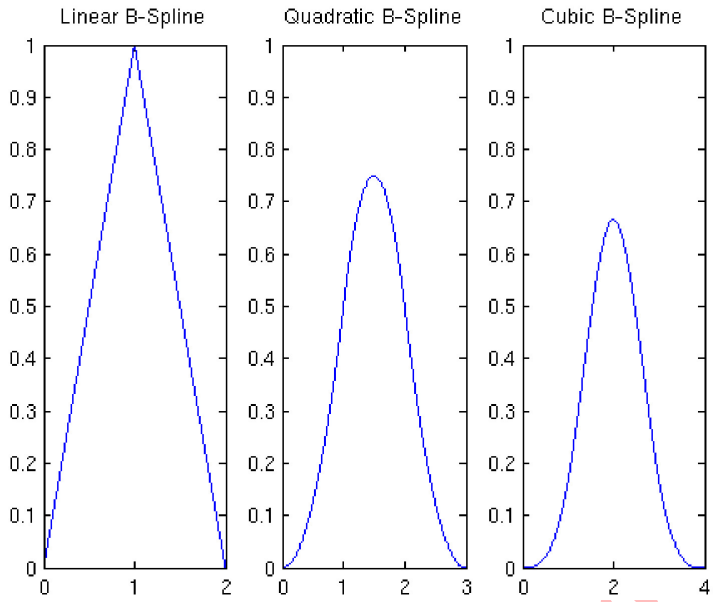

FIGURE 1. Graph of b^1, b^2 and b^3.

- We discuss the existence and uniqueness of the solution for the considered problem. Additionally, we also derive the regularity results.
- A unified mesh-free scheme is proposed that is based on $L1$ and $L2\text{-}1_\sigma$ methods along with weighted b-splines. Newton's method is utilized to handle the nonlinearity in the scheme.
- We establish α-robust estimates for the fully-discrete solution in both $L^2(\Omega)$ and $H_0^1(\Omega)$ norms.
- The theoretical estimates are validated through three numerical experiments conducted on different domains.

To the best of our knowledge, this is the first attempt to numerically solve problem (1.1) using a weighted b-spline based mesh-free method combined with $L1$ and $L2\text{-}1_\sigma$ schemes on a graded mesh.

The paper is organized as follows: Section 2 covers the construction of a finite element basis with a weighted b-spline. Section 3 discusses the existence, uniqueness, and regularity of a weak solution at a continuous level. Section 4 proposes the fully-discrete scheme for solving the time-fractional nonlocal Equation (1.1) that uses $L1$ and $L2\text{-}1_\sigma$ methods on a graded mesh for time discretization, and weighted b-splines for spatial discretization. We obtain α-robust *a priori* bounds and convergence results for the numerical solution of the proposed scheme. Section 5 presents comparative numerical simulations of a mesh-free weighted b-spline method with a standard FEM. Finally, we conclude the paper in Section 6.

2. Weighted b-Spline Basis

In this section, we outline the procedure for constructing weighted b-spline basis functions, as described in [13, 14]. This process incorporates the concepts of weight functions and b-splines. We begin by defining the b-splines. For a knot sequence $0, 1, \ldots, m+1$, the recursion formula for standard uniform b-spline of degree m is given below [13]:

$$b^m(x) = \frac{x}{m} b^{m-1}(x) + \frac{m+1-x}{m} b^{m-1}(x-1), \tag{2.1}$$

where b^0 is defined as the characteristic function in the interval $[0, 1]$, i.e., $b^0(x) = \chi_{[0,1]}(x)$. In Figure 1, we have shown the graph of linear (b^1), quadratic (b^2) and cubic (b^3) b-splines.

The uniform b-spline b_k in d dimension is constructed by taking the product of scale and the translate of univariate b-splines [14]:

$$b_k(x) = \prod_{i=1}^{d} b^m \left(\frac{x_i}{h} - k_i \right), \ k \in \mathbb{Z}^d, \tag{2.2}$$

where h is grid width, $k = (k_1, k_2, \ldots, k_d)$, $x = (x_1, x_2, \ldots, x_d)$, and b^m is the standard univariate cardinal b-spline of degree m. These b-spline b_k, $k \in \mathbb{Z}^d$ are nonnegative, C^{m-1} smooth with support $supp(b_k) = kh + [0, m+1]^d h$. On each grid cell $Q_l = lh + [0,1]^d h$, $l \in \mathbb{Z}^d$ b-splines b_k are polynomials of degree m in each variable. Those b-splines that have some support in Ω are referred to as relevant b-splines otherwise, they are considered irrelevant b-splines. We can define the spline space $\mathbb{S}$ spanned by all relevant b-splines and write $\mathbb{S} = span\{b_k : k \in S\}$, where S is the relevant index set for domain Ω. For computations, it is convenient to keep irrelevant indices as well, which means we can write the approximate solution in the following form:

$$\sum_{k \in S'} u_k b_k,$$

where $S^{'}$ the smallest rectangular array containing all relevant indices k, and the coefficients u_k are set to zero for $k \notin S$. There are two primary reasons for b-splines space not to be used as a finite element space. The first one is that b-splines, in general, do not conform to the essential boundary condition. Secondly, b-splines do not provide a stable basis for finite element approximation Ω [12, 14]. Indeed, one way to resolve the issue related to essential boundary condition is by multiplying a positive weight function w to the b-splines, which vanishes on the boundary $\partial\Omega$ [12–14, 26]. To be more precise, a weight function w associated with a part Γ of the boundary of the simulation domain Ω has bounded gradient, is positive in Ω, and vanishes on Γ [14].

Weight functions can be determined analytically for particular domains, such as circles, squares, etc. For complex domains, various methods are available for constructing the weight functions w (see [12, 13] for more details). The stability issue was examined by K. Höllig et al. in [12] through the extension procedure. In contrast, the authors in [14] demonstrated that accurate approximation is possible without incorporating the extension procedure. Therein authors mentioned that the preconditioning techniques are adequate for effectively solving the ill-conditioned Galerkin matrix system with acceptable precision. In the following, now we introduce the weighted b-spline space [14]:

$$B_h = span\{wb_k : k \in S\}.$$

3. Well-posedness and Regularity of the Solution

Definition 3.1. The weak solution u of the problem (1.1) is such that $u(\cdot, t) \in H_0^1(\Omega)\ \forall\ t \in (0, T]$ and the following equation holds for a.e. $t \in (0, T]$

$$({}_0^c D_t^\alpha u, \psi) + M\left(\int_\Omega u\, dx \right) (\nabla u, \nabla \psi) = (f, \psi), \tag{3.1}$$

$$\big(u(\cdot, 0), \psi\big) = \big(u_0(\cdot), \psi\big) \quad \forall\ \psi \in H_0^1(\Omega). \tag{3.2}$$

The following assumptions have been made on the problem data, similar to [4], to ensure the existence and uniqueness of a weak solution:
$H1$: $u_0 \in H_0^1(\Omega) \cap H^2(\Omega)$, $f \in L^\infty(0, T; L^2(\Omega))$.
$H2$: $M : \mathbb{R} \longrightarrow \mathbb{R}_+$ is such that

$$\infty > m_2 \geq M(s) \geq m_1 > 0, \quad \forall s \in \mathbb{R}. \tag{3.3}$$

$H3$: M is a Lipschitz continuous function, i.e., $|M(u_1) - M(u_2)| \leq L_M |u_1 - u_2|$ for all $u_1,\ u_2 \in \mathbb{R}$, where L_M is a positive constant. It can be shown that under assumptions $H1$-$H3$, the considered problem (3.1) has a unique weak solution that satisfies $\|u\|_{L^\infty(0,T;L^2(\Omega))} \leq C$ [22]. In this work, we take C as a generic constant that may depend on various parameters but is always independent of spatial and temporal step sizes.

We now mention some notations that are required to discuss the regularity of the solution for the time-fractional nonlocal diffusion equation (see Chapter 3 of [31]). For $\mu \geq 0$, we denote $\dot{H}^{\mu}$ as a subspace of $L^2(\Omega)$ such that

$$\dot{H}^{\mu}(\Omega) = \{v \in L^2(\Omega) : \sum_{k=1}^{\infty} \Lambda_k^{\mu} |(v, \Psi_k)|^2 < \infty\}. \tag{3.4}$$

The norm in $\dot{H}^{\mu}(\Omega)$ is given by

$$|v|_{\mu}^2 = \sum_{k=1}^{\infty} \Lambda_k^{\mu} |(v, \Psi_k)|^2, \tag{3.5}$$

where $(\cdot, \cdot)$ denote the $L^2(\Omega)$ inner product. Here, $\{\Lambda_k\}_{k=1}^{\infty}$ and $\{\Psi_k\}_{k=1}^{\infty}$ denote eigenvalues and orthonormal eigenfunctions respectively of the eigen value problem $-\Delta\Psi = \Lambda\Psi$ in Ω with $\Psi = 0$ on $\partial\Omega$. Note that eigenfunctions $\{\Psi_k\}_{k=1}^{\infty}$ forms an orthonrmal basis of $L^2(\Omega)$ and eigenvalues are positive such that $0 < \Lambda_1 \leq \Lambda_2 \leq \cdots \leq \Lambda_k \leq \ldots$ and each of which has finite multiplicity.
In particular, if $\mu = 0$, $|v|_0 = \|v\| = (v, v)^{1/2}$ is the $L^2(\Omega)$ norm and if $\mu = 1$, $|v|_1 = \|\nabla v\|$ is the $H_0^1(\Omega)$ norm. Furthermore, if $\mu = 2$, $|v|_2 = \|\Delta v\|$ is the equivalent norm in $H^2(\Omega) \cap H_0^1(\Omega)$. Thus $\dot{H}^0(\Omega) = L^2(\Omega)$, $\dot{H}^1(\Omega) = H_0^1(\Omega)$, and $\dot{H}^2(\Omega) = H^2(\Omega) \cap H_0^1(\Omega)$. For general $\mu \in \mathbb{N} \cup \{0\}$, the space

$$\dot{H}^{\mu}(\Omega) = \left\{ v \in H^{\mu};\ \Delta^k v = 0 \text{ on } \partial\Omega,\ \text{for each non-negative integer } k < \frac{\mu}{2} \right\}. \tag{3.6}$$

Moreover, both norms $|v|_{\mu} = \|\cdot\|_{\dot{H}^{\mu}(\Omega)}$ and $\|\cdot\|_{H^{\mu}(\Omega)}$ are equivalent in $\dot{H}^{\mu}(\Omega)$.

Theorem 3.2. *If $u_0 \in \dot{H}^2(\Omega)$ and $f \in L^{\infty}(0, T; \dot{H}^2(\Omega))$, then the solution u of problem (1.1) satisfies the following regularity estimates for all $t \in [0, T]$ and all $t_1, t_2 \in [0, T]$:*

$$\|u(t)\|_{H^2(\Omega)} \leq C, \quad \|{}_0^c D_t^{\alpha} u(t)\| \leq C, \quad \text{and} \quad \|u(t_2) - u(t_1)\| \leq C|t_2 - t_1|^{\alpha}.$$

Proof. Consider the weak formulation (3.1) as

$$({}_0^c D_t^{\alpha} u, \psi) + M\left(\int_{\Omega} u\, dx\right)(-\Delta u, \psi) = (f(\cdot, t), \psi), \quad \forall \psi \in V,\ a.e.\ t \in [0, T], \tag{3.7}$$

$$u(x, 0) = u_0. \tag{3.8}$$

With the help of an orthonormal basis $\{\Psi_k\}_{k=1}^{\infty}$, the solution u of the problem can be expressed as a Fourier series expansion by

$$u(x, t) = \sum_{k=1}^{\infty} \gamma_k(t) \Psi_k(x). \tag{3.9}$$

Further, by employing this expansion (3.9) in (3.7) along with $\psi = \Psi_k$, one has

$${}_0^c D_t^{\alpha} \gamma_k(t) = -\Lambda_k M\left(\int_{\Omega} u\, dx\right) \gamma_k(t) + (f(\cdot, t), \Psi_k)$$

$$\gamma_k(0) = (u_0, \Psi_k), \forall\ k = 1, 2, \ldots.$$

We obtain the following integral equation with a weakly singular kernel while applying the fractional-integral operator of order α on both sides

$$\gamma_k(t) = \gamma_k(0) - \frac{\Lambda_k}{\Gamma(\alpha)} \int_0^t (t - s)^{\alpha - 1} M\left(\int_{\Omega} u(x, s)\, dx\right) \gamma_k(s) ds$$

$$+ \frac{1}{\Gamma(\alpha)} \int_0^t (t - s)^{\alpha - 1} (f(\cdot, s), \Psi_k) ds.$$

Utilizing $\|u\|_{L^{\infty}(0,T;L^2(\Omega))} \leq C$ and $H2$ to get

$$|\gamma_k(t)| \leq |\gamma_k(0)| + \frac{\Lambda_k m_2}{\Gamma(\alpha)} \int_0^t (t - s)^{\alpha - 1} |\gamma_k(s)| ds + \frac{T^{\alpha}}{\Gamma(1 + \alpha)} \left| \left(\sup_{s \in [0,T]} f(\cdot, s), \Psi_k \right) \right|, \ \forall\ k = 1, 2, \ldots.$$

The Gronwall inequality [32] gives

$$|\gamma_k(t)| \leq C\left(|\gamma_k(0)| + \frac{T^\alpha}{\Gamma(1+\alpha)}\left|\left(\sup_{s\in[0,T]} f(\cdot,s), \Psi_k\right)\right|\right) E_\alpha(\Lambda_k m_2 t^\alpha) \tag{3.10}$$

$$\leq C\left(|(u_0,\Psi_k)| + \left|\left(\sup_{s\in[0,T]} f(\cdot,s), \Psi_k\right)\right|\right). \tag{3.11}$$

Now, for $\mu = 0,\ 1$, and 2 the Equation (3.5) gives

$$|u|_\mu^2 = \sum_{k=1}^{\infty} \Lambda_k^\mu |(u,\Psi_k)|^2 = \sum_{k=1}^{\infty} \Lambda_k^\mu |\gamma_k(t)|^2.$$

Using (3.10), we get

$$|u|_\mu^2 \leq C\left[\sum_{k=1}^{\infty} \Lambda_k^\mu |(u_0,\Psi_k)|^2 + \sum_{k=1}^{\infty} \Lambda_k^\mu \left|\left(\sup_{s\in[0,T]} f(\cdot,s), \Psi_k\right)\right|^2\right]. \tag{3.12}$$

The definition of norm given in (3.5) and $\left|\sup_{s\in[0,T]} f(\cdot,s)\right|^2 \leq \sup_{s\in[0,T]} (|f(\cdot,s)|^2)$ provide

$$|u|_\mu^2 \leq C\big(|u_0|_\mu^2 + \|f\|^2_{L^\infty(0,T;\dot{H}^\mu(\Omega))}\big)\ \forall\ t\in[0,T].$$

By combining the results for $\mu = 0, 1$, and 2, we get

$$\|u(t)\|_{H^2(\Omega)} \leq C\big(\|u_0\|_{H^2(\Omega)} + \|f\|_{L^\infty(0,T;H^2(\Omega))}\big),\ \forall\ t\in[0,T]. \tag{3.13}$$

Next, to derive the second result of the theorem, we consider the given equation as

$${}_0^c D_t^\alpha u = M\left(\int_\Omega u\,dx\right)\Delta u + f(x,t)$$

From above equation, we can get the following estimate

$$\|{}_0^c D_t^\alpha u(t)\| \leq m_2\|\Delta u(t)\| + \|f\|_{L^\infty(0,T;L^2(\Omega))}. \tag{3.14}$$

Equations (3.14) and (3.13) together yield the desired result for ${}_0^c D_t^\alpha u$.
Next, we notice that the solution u of the considered problem (1.1) satisfies the following integral equation

$$u(t) = u_0 + \frac{1}{\Gamma(\alpha)}\int_0^t (t-s)^{\alpha-1} M\left(\int_\Omega u(x,s)\,dx\right)\Delta u(s)ds + \frac{1}{\Gamma(\alpha)}\int_0^t (t-s)^{\alpha-1} f(s)ds. \tag{3.15}$$

Now, let $t_1 < t_2$ (without loss of generality), and then from (3.15) we get

$$\begin{aligned} u(t_2) - u(t_1) = &\frac{1}{\Gamma(\alpha)}\int_0^{t_2} (t_2-s)^{\alpha-1} M\left(\int_\Omega u(x,s)\,dx\right)\Delta u(s)ds \\ &+ \frac{1}{\Gamma(\alpha)}\int_0^{t_2} (t_2-s)^{\alpha-1} f(s)ds \\ &- \frac{1}{\Gamma(\alpha)}\int_0^{t_1} (t_1-s)^{\alpha-1} M\left(\int_\Omega u(x,s)\,dx\right)\Delta u(s)ds \\ &- \frac{1}{\Gamma(\alpha)}\int_0^{t_1} (t_1-s)^{\alpha-1} f(s)ds. \end{aligned} \tag{3.16}$$

The Equation (3.16) produces

$$\begin{aligned} u(t_2) - u(t_1) = &\frac{1}{\Gamma(\alpha)}\int_0^{t_1} \big((t_2-s)^{\alpha-1} - (t_1-s)^{\alpha-1}\big) M\left(\int_\Omega u(x,s)\,dx\right)\Delta u(s)ds \\ &+ \frac{1}{\Gamma(\alpha)}\int_{t_1}^{t_2} (t_2-s)^{\alpha-1} M\left(\int_\Omega u(x,s)\,dx\right)\Delta u(s)ds \end{aligned}$$

$$+\frac{1}{\Gamma(\alpha)}\int_0^{t_1}\big((t_2-s)^{\alpha-1}-(t_1-s)^{\alpha-1}\big)f(s)ds$$
$$+\frac{1}{\Gamma(\alpha)}\int_{t_1}^{t_2}(t_2-s)^{\alpha-1}f(s)ds. \tag{3.17}$$

Hence, from (3.17), we have

$$\|u(t_2)-u(t_1)\|\le C\bigg[\int_0^{t_1}\big|(t_2-s)^{\alpha-1}-(t_1-s)^{\alpha-1}\big|ds+\int_{t_1}^{t_2}(t_2-s)^{\alpha-1}ds\bigg]. \tag{3.18}$$

Notice that $(t_2-s)^{\alpha-1}-(t_2-s)^{\alpha-1}$ is negative. Thus, use this fact in (3.18) to achieve

$$\begin{aligned}\|u(t_2)-u(t_1)\|\le&C\bigg[\int_0^{t_1}\big((t_1-s)^{\alpha-1}-(t_2-s)^{\alpha-1}\big)ds+\int_{t_1}^{t_2}(t_2-s)^{\alpha-1}ds\bigg]\\ =&C\big[(t_2-t_1)^{\alpha}+t_1^{\alpha}-t_2^{\alpha}+(t_2-t_1)^{\alpha}\big].\end{aligned}$$

Since $t_1^{\alpha}-t_2^{\alpha}<0$, therefore

$$\|u(t_2)-u(t_1)\|\le C|t_2-t_1|^{\alpha}\ \forall\ \ t_1,t_2\in[0,T].$$

This complete the proof. □

Remark 3.3. The above theorem proves that the solution u of time-fractional nonlocal diffusion equation satisfies $u\in L^{\infty}(0,T;H^2(\Omega))\cap C^{\alpha}(0,T;L^2(\Omega))$ and ${}_0^cD_t^{\alpha}u\in L^{\infty}(0,T;L^2(\Omega))$ under the regularity assumptions $u_0\in\dot{H}^2(\Omega)$ and $f\in L^{\infty}(0,T;\dot{H}^2(\Omega))$ on problem data. Similar argument follows to prove that for any $\mu\in\mathbb{N}\cup\{0\}$, if $u_0\in\dot{H}^{\mu+2}(\Omega))$ and $f\in L^{\infty}(0,T;\dot{H}^{\mu+2}(\Omega))$, then $u\in L^{\infty}(0,T;\dot{H}^{\mu+2}(\Omega))\cap C^{\alpha}(0,T;\dot{H}^{\mu})$ and ${}_0^cD_t^{\alpha}u\in L^{\infty}(0,T;\dot{H}^{\mu})$. It is important to note that the boundary condition given in the definition of $\dot{H}^{\mu}(\Omega)$ (in Equation (3.6)) is restrictive as it can be seen from the example of a smooth function $v=(1-x)(1-y)xy$ defined on $\Omega=(0,1)\times(0,1)$. Here, $v\in\dot{H}^2(\Omega)$ but does not belong $\dot{H}^3(\Omega)$ because its Laplacian $\Delta v=-2(1-x)x-2(1-y)y$ does not vanish on the boundary of the domain Ω. The assumption of more regularity on data can lead to severe restrictions on the considered problem. Note that this work proves $C^{\alpha}[0,T]$ regularity for the time variable and general regularity results require further attention from academicians.

4. A Unified Fully-Discrete Scheme

For the fully-discrete formulation, we consider a partition of $[0,T]$ given by $0=t_0<t_1<\cdots<t_N=T$, where $t_n=T\left(\frac{n}{N}\right)^r$ for $n=0,1,\ldots,N$. Here, $r\ge1$ is the grading parameter, and $N\in\mathbb{N}$. Let $\sigma\in[0,1]$ be a constant, and define $t_{n-\sigma}$ as $t_{n-\sigma}:=\sigma t_{n-1}+(1-\sigma)t_n$. Now, we denote the exact solution of the given problem (1.1) by u^n and the corresponding fully-discrete solution by U_h^n at $t=t_n$. Next, the approximation of the Caputo fractional derivative in a unified manner can be given by the following general formula:

$$\begin{aligned}{}_0^cD_{t_{n-\sigma}}^{\alpha}\rho\ \approx&D_N^{\alpha}\rho^{n-\sigma}\\ :=&\sum_{j=1}^{n}\mathcal{B}_{\sigma,n-j}^{n}(\rho^j-\rho^{j-1})\quad\text{for } 1\le n\le N.\end{aligned} \tag{4.1}$$

For different choices of σ and $\mathcal{B}_{\sigma,n-j}^{n}$, the general formula (4.1) will reduce to the following approximations.
L1 **approximation [30]:** For $\sigma=0$, the discrete coefficient $\mathcal{B}_{\sigma,n-j}^{n}$ in (4.1) is given by

$$\mathcal{B}_{\sigma,n-j}^{n}=\frac{1}{\Gamma(1-\alpha)}\int_{t_{j-1}}^{t_j}\frac{(t_n-\eta)^{-\alpha}}{\tau_j}\,d\eta\ \text{ for } n\ge1 \text{ and } 1\le j\le n,$$

where $\tau_j=t_j-t_{j-1}$.
L2-1$_\sigma$ **approximation [16]:** The values of discrete coefficients $\mathcal{B}_{\sigma,n-j}^{n}$ in (4.1) are given below:

$$\text{for } n=1,\ \mathcal{B}_{\sigma,0}^{1}=a_{1,0}$$

and

$$\text{for } n \geq 2,\ \mathcal{B}^n_{\sigma,n-j} = \begin{cases} a_{n,0} + \frac{\tau_{n-1}}{\tau_n} b_{n,1}, & \text{if } j = n, \\ a_{n,n-j} + \frac{\tau_{j-1}}{\tau_j} b_{n,n-j+1} - b_{n,n-j}, & \text{if } 2 \leq j \leq n-1, \\ a_{n,n-1} - b_{n,n-1}, & \text{if } j = 1, \end{cases}$$

where

$$a_{n,0} = \frac{\tau_n^{-1}}{\Gamma(1-\alpha)} \int_{t_{n-1}}^{t_{n-\sigma}} (t_{n-\sigma} - \eta)^{-\alpha} d\eta,$$

$$a_{n,n-j} = \frac{\tau_j^{-1}}{\Gamma(1-\alpha)} \int_{t_{j-1}}^{t_j} (t_{n-\sigma} - \eta)^{-\alpha} d\eta \quad \text{for } 1 \leq j \leq n-1,$$

$$b_{n,n-j} = \frac{2\tau_j^{-1}}{\Gamma(1-\alpha)(t_{j+1} - t_{j-1})} \int_{t_{j-1}}^{t_j} (t_{n-\sigma} - \eta)^{-\alpha} (\eta - t_{j-\frac{1}{2}}) d\eta \quad \text{for } 1 \leq j \leq n-1.$$

Now, the fully-discrete scheme seeks the solution $U_h^n \in B_h$ such that for each $n = 1, 2, \ldots, N$, one has

$$(D_N^\alpha U_h^{n-\sigma}, \psi_h) + M\left(\int_\Omega U_h^{n,\sigma}\, dx \right) (\nabla U_h^{n,\sigma}, \nabla \psi_h) = (f^{n-\sigma}, \psi_h) \quad \forall\ \psi_h \in B_h \tag{4.2}$$

and

$$U_h^0 = u_h^0 \quad \text{for} \quad n = 0, \tag{4.3}$$

where $U_h^{n,\sigma} = (1-\sigma) U_h^n + \sigma U_h^{n-1}$ and u_h^0 is some approximation of u_0. Let $\{\phi_i : 1 \leq i \leq N_d\}$ be the basis of finite dimensional space B_h, then the solution $U_h^n \in B_h$ of the scheme (4.2) can be written in a linear combination of basis functions with $\alpha_i^n \in \mathbb{R}$ as $U_h^n = \sum_{i=1}^{N_d} \alpha_i^n \phi_i$. Further, if we substitute this into the equation (4.2) and utilize Newton's method to solve the resulting nonlinear system of equations, we encounter a dense Jacobian matrix [4]. To address this concern, we adopt the approach proposed in the references [4, 10]. Now, we modify problem (4.2) such that, for $d \in \mathbb{R}$ and $U_h^n \in B_h$ the following holds:

$$\int_\Omega U_h^{n,\sigma}\, dx - d = 0, \tag{4.4}$$

$$(D_N^\alpha U_h^{n-\sigma}, \psi_h) + M(d)(\nabla U_h^{n,\sigma}, \nabla \psi_h) = (f^{n-\sigma}, \psi_h) \quad \forall\ \psi_h \in B_h. \tag{4.5}$$

Note that problem (4.4)-(4.5) and problem (4.2) are equivalent [4] in the sense that the solution of one will be the solution of another. Next we choose $\psi_h = \phi_j$ and rewrite the Equations (4.4)-(4.5) as

$$F_j(U_h^n, d) = (D_N^\alpha U_h^{n-\sigma}, \phi_j) + M(d)(\nabla U_h^{n,\sigma}, \nabla \phi_j) - (f^{n-\sigma}, \phi_j) \text{ for } 1 \leq j \leq N_d, \tag{4.6}$$

$$F_{N_d+1} = \int_\Omega U_h^{n,\sigma}\, dx - d. \tag{4.7}$$

An application of Newton's method in (4.6)-(4.7) gives rise to the following matrix equation [5].

$$J \begin{bmatrix} \bar{\alpha}^n \\ \beta \end{bmatrix} = \begin{bmatrix} A & b \\ c & \delta_{11} \end{bmatrix} \begin{bmatrix} \bar{\alpha}^n \\ \beta \end{bmatrix} = \begin{bmatrix} \bar{F} \\ F_{N_d+1} \end{bmatrix},$$

where J is the sparse Jacobian matrix, $\bar{\alpha}^n = [\alpha_1^n, \alpha_2^n, \ldots, \alpha_{N_d}^n]'$, $\bar{F} = [F_1, F_2, \ldots, F_{N_d}]'$ and entries A, b and c are given below:

$$A_{jl} = \mathcal{B}^n_{\sigma,0}(\phi_l, \phi_j) + (1-\sigma) M(d)(\nabla \phi_l, \nabla \phi_j), \quad \text{for } 1 \leq l, j \leq N_d, \tag{4.8}$$

$$b_{j1} = M'(d)(\nabla U_h^{n,\sigma}, \nabla \phi_j) \text{ for } 1 \leq j \leq N_d, \tag{4.9}$$

$$c_{1l} = (1-\sigma) \int_\Omega \phi_l\, dx \text{ for } 1 \leq l \leq N_d, \tag{4.10}$$

$$\delta_{11} = -1. \tag{4.11}$$

Now, in our further numerical analysis of the proposed scheme, we require some more results and notations.

Lemma 4.1. *[1] Let the function $v^k = v(\cdot, t^k) \in L^2(\Omega)$ for $k = 0, 1, 2, \ldots, N$. Then it satisfies:*

$$\left(D_N^{\alpha} v^{n-\sigma},\, v^{n,\sigma}\right) \geq \frac{1}{2} D_N^{\alpha} \|v^{n-\sigma}\|^2 \text{ for } n = 1, 2, \ldots, N. \tag{4.12}$$

Next, we define the discrete Laplacian operator $\Delta_h : B_h \to B_h$ such that the following holds [31]:

$$(-\Delta_h \bar{u}, v) := (\nabla \bar{u}, \nabla v) \quad \forall\ \bar{u},\ v \in B_h \tag{4.13}$$

Further, for $n = 1, 2, \ldots, N$, the discrete coefficients $Q_{n-i}^{(n)}$ are defined as follows:

$$Q_{n-i}^{(n)} := \begin{cases} \frac{1}{\mathcal{B}_{\sigma,0}^{i}} \sum_{k=i+1}^{n} \left(\mathcal{B}_{\sigma,k-i-1}^{k} - \mathcal{B}_{\sigma,k-i}^{k}\right) Q_{n-k}^{(n)}, & \text{if } 1 \leq i \leq n-1, \\ \frac{1}{\mathcal{B}_{\sigma,0}^{n}}, & \text{if } i = n. \end{cases}$$

Lemma 4.2. *[6] If the constant $\gamma \in (0, 1)$, then one has*

$$\sum_{j=1}^{n} Q_{n-j}^{(n)} j^{r(\gamma-\alpha)} \leq \frac{\pi_A \Gamma(1+\gamma-\alpha)}{\Gamma(1+\gamma)} T^{\alpha} \left(\frac{t_n}{T}\right)^{\gamma} N^{r(\gamma-\alpha)}, \quad \text{for } n = 1, 2, \ldots, N,$$

where $\pi_A = \frac{11}{4}$ for $\sigma = \frac{\alpha}{2}$ and $\pi_A = 1$ for $\sigma = 0$.

Next, we state the discrete fractional Gronwall inequality that provides α-robust estimates for the fully-discrete solution U_h^n.

Lemma 4.3. *[16] Let $0 \leq \gamma \leq 1$, $\lambda_l \geq 0$, and Λ be constants such that $\sum_{l=0}^{n} \lambda_l \leq \Lambda$ for $n \geq 1$. Suppose the nonnegative sequences $\{\zeta^n\}$, $\{\eta^n\}$ are bounded, and the grid function $\{\omega^n \geq 0,\ \text{for } n \geq 0\}$ satisfy the inequality for $n = 1, 2, \ldots, N$,*

$$D_N^{\alpha} \left[(\omega^{n-\gamma})^2\right] \leq \sum_{k=1}^{n} \lambda_{n-k} \left(\omega^{k,\theta_1}\right)^2 + \zeta^n \omega^{k,\theta_2} + (\eta^n)^2$$

where $\omega^{k,\theta_i} := \theta_i \omega^{k-1} + (1-\theta_i)\omega^k$ for $\theta_i \in [0,1]$ and $i, = 1, 2$.
Then

$$\omega^n \leq 2E_{\alpha}\left(2\pi_A \Lambda\, t_n^{\alpha}\right) \left[\omega^0 + \max_{1 \leq k \leq n} \sum_{j=1}^{k} Q_{k-j}^{(k)} (\zeta^j + \eta^j) + \max_{1 \leq k \leq n} \{\eta^k\}\right],$$

provided that the maximum time-step $\tau_N \leq \frac{1}{\sqrt[\alpha]{2\pi_A\, \Gamma(2-\alpha)\, \Lambda}}$.

Here, $E_{\alpha}(z) := \sum_{k=0}^{\infty} \frac{z^k}{\Gamma(1+k\alpha)}$ is the Mittag-Leffler function, and $\pi_A = \frac{11}{4}$ for $\sigma = \frac{\alpha}{2}$, while $\pi_A = 1$ for $\sigma = 0$.

Theorem 4.4. *If U_h^n is the solution of the problem (4.2) then for each $n = 1, 2, \ldots, N$, U_h^n satisfy following estimates:*

$$\max_{1 \leq n \leq N} \|U_h^n\| \leq C\left(1 + \|U_h^0\|\right), \tag{4.14a}$$

$$\max_{1 \leq n \leq N} \|\nabla U_h^n\| \leq C\left(1 + \|\nabla U_h^0\|\right). \tag{4.14b}$$

Proof. Taking $\psi_h = U_h^{n,\sigma}$ in (4.2), we get

$$\left(D_N^{\alpha} U_h^{n-\sigma}, U_h^{n,\sigma}\right) + M\left(\int_{\Omega} U_h^{n,\sigma}\, dx\right) \left(\nabla U_h^{n,\sigma}, \nabla U_h^{n,\sigma}\right) = \left(f^{n-\sigma}, U_h^{n,\sigma}\right). \tag{4.15}$$

By using Lemma 4.1, assumption $H2$, Young's and Cauchy-Schwarz inequalities in (4.15), we get

$$\frac{1}{2} D_N^{\alpha} \|U_h^{n-\sigma}\|^2 \leq \frac{1}{2} \|f^{n-\sigma}\|^2 + \frac{1}{2} \|U_h^{n,\sigma}\|^2. \tag{4.16}$$

Now, we can use Lemma 4.3 and Lemma 4.2 (with $\gamma = \alpha$) in (4.16) to get the first desired result. Similarly, by taking the test function $\psi_h = -\Delta_h U_h^{n,\sigma}$ in (4.2), we can prove the bound (4.14b). □

We now state some regularity assumptions on the solution u, along with some notations and results from [17] that are required to obtain error estimates for the fully-discrete solution U_h^n :

$$\|{}_0^c D_t^\alpha u\|_{L^\infty(0,T;H_0^1(\Omega)\cap H^{m+2}(\Omega))} \le C, \quad \|u\|_{L^\infty(0,T;H_0^1(\Omega)\cap H^{m+2}(\Omega))} \le C, \quad \text{and} \tag{4.17}$$

$$\|\partial_t^p u(\cdot,t)\|_{H^2(\Omega)} \le C(1+t^{\alpha-p}) \quad \text{for} \quad 0 < t \le T, \ \text{where } p = 0,\ 1,\ 2,\ 3. \tag{4.18}$$

The L^2-projection $P_h : L^2(\Omega) \to B_h$ is defined as follows:

$$(u, v_h) = (P_h u, v_h) \quad \forall\ u \in L^2(\Omega) \text{ and } v_h \in B_h. \tag{4.19}$$

Moreover, the H^1 stability result holds for the projection P_h, i.e.,

$$\|\nabla P_h u\| \le C\|\nabla u\| \quad \forall\ u \in H_0^1(\Omega). \tag{4.20}$$

Further, the Ritz-projection $R_h : H_0^1(\Omega) \to B_h$ as follows:

$$(\nabla \bar{u}, \nabla v_h) = (\nabla R_h \bar{u}, \nabla v_h) \quad \forall\ \bar{u} \in H_0^1(\Omega) \text{ and } v_h \in B_h. \tag{4.21}$$

Lemma 4.5. *[16] Let $\omega \in C[0,T]\cap C^3(0,T]$. Assume $\|\partial_t^p \omega(t)\|_2 \le C(1+t^{\alpha-p})$ for $p = 0,1,2,3$ and $0 < t \le T$. Then following inequality holds:*

$$\|{}_0^c D^\alpha_{t_{n-\sigma}}\omega - D_N^\alpha\, \omega^{n-\sigma}\|_{H^1(\Omega)} \le \begin{cases} C t_{n-\sigma}^{-\alpha}\, N^{-\min\{3-\alpha,\, r\alpha\}}, & \text{if } \sigma = \frac{\alpha}{2}, \\ C t_n^{-\alpha}\, N^{-\min\{2-\alpha,\, r\alpha\}}, & \text{if } \sigma = 0. \end{cases}$$

Lemma 4.6. *[16] Let $\omega \in C^2(0,T]$. For $p = 0,1,2$ and $0 < t \le T$, let $\|\partial_t^p \omega(t)\|_2 \le C\,(1+t^{\alpha-p})$. Then, we have*

$$\|\omega^{n,\sigma} - \omega^{n-\sigma}\|_{H^2(\Omega)} \le \begin{cases} C N^{-\min\{r\alpha,\, 2\}}, & \text{if } \sigma = \frac{\alpha}{2}, \\ 0, & \text{if } \sigma = 0. \end{cases}$$

The Ritz projection R_h satisfies the following estimate in more general spaces.

Theorem 4.7. *[3, 31] For $l = 0,1$ and $l < k \le m+1$, there exists constant C such that*

$$||\chi(t)||_{H^l(\Omega)} \le C h^{k-l} ||u(t)||_{H^k(\Omega)} \quad \forall\ u(t) \in H^k(\Omega)\cap H_0^1(\Omega),$$

where $\chi(t) = u(t) - R_h u(t)$.

In the following theorem, we establish convergence results of the fully-discrete solution. For this purpose, we rewrite the error $u(t_n) - U_h^n$ using the Ritz projection R_h as

$$u(t_n) - U_h^n = (u(t_n) - R_h u(t_n)) + (R_h u(t_n) - U_h^n) \tag{4.22}$$

$$= \chi^n + \eta^n. \tag{4.23}$$

4.1. Weighted b-splines Based Error Estimates.

Theorem 4.8. *Let u^n be the exact solution and U_h^n be the approximate solution of problems (1.1) and (4.2) respectively, then the following estimates hold for $1 \le n \le N$*

$$\max_{1\le n\le N} \|u^n - U_h^n\| \le \begin{cases} C\big(h^{m+1} + N^{-\min\{2,\, r\alpha\}}\big), & \text{if } \sigma = \frac{\alpha}{2}, \\ C\big(h^{m+1} + N^{-\min\{2-\alpha,\, r\alpha\}}\big), & \text{if } \sigma = 0, \end{cases} \tag{4.24a}$$

$$\max_{1\le n\le N} \|\nabla u^n - \nabla U_h^n\| \le \begin{cases} C\big(h^{m} + N^{-\min\{2,\, r\alpha\}}\big), & \text{if } \sigma = \frac{\alpha}{2}, \\ C\big(h^{m} + N^{-\min\{2-\alpha,\, r\alpha\}}\big), & \text{if } \sigma = 0. \end{cases} \tag{4.24b}$$

Proof. For any $\psi_h \in B_h$, the estimate for η^n is given by

$$\begin{aligned}\left(D_N^\alpha \eta^{n-\sigma}, \psi_h\right) + M\left(\int_\Omega U_h^{n,\sigma}\, dx\right)\left(\nabla\eta^{n,\sigma}, \nabla\psi_h\right) &= \left(D_N^\alpha R_h u^{n-\sigma}, \psi_h\right) + M\left(\int_\Omega U_h^{n,\sigma}\, dx\right)\left(\nabla R_h u^{n,\sigma}, \nabla\psi_h\right)\\ &\quad - \left(D_N^\alpha U_h^{n-\sigma}, \psi_h\right) - M\left(\int_\Omega U_h^{n,\sigma}\, dx\right)\left(\nabla U_h^{n,\sigma}, \nabla\psi_h\right)\\ &= \left(D_N^\alpha R_h u^{n-\sigma} - {}_0^c D_{t_{n-\sigma}}^\alpha u, \psi_h\right)\\ &\quad - M\left(\int_\Omega u^{n-\sigma} dx\right)\left(\Delta u^{n,\sigma} - \Delta u^{n-\sigma}, \psi_h\right)\\ &\quad - \left(M\left(\int_\Omega U_h^{n,\sigma}\, dx\right) - M\left(\int_\Omega u^{n-\sigma}\, dx\right)\right)\left(\Delta u^{n,\sigma}, \psi_h\right).\end{aligned} \tag{4.25}$$

Choosing $\psi_h = \eta^{n,\sigma}$ in (4.25) then use Cauchy-Schwarz inequality, triangle inequality, Lemma 4.1 and assumption $H2$ to get

$$\begin{aligned}\frac{1}{2} D_N^\alpha \|\eta^{n-\sigma}\|^2 + m_1 \|\nabla\eta^{n,\sigma}\|^2 \le \Big(&\|D_N^\alpha R_h u^{n-\sigma} - {}_0^c D_{t_{n-\sigma}}^\alpha R_h u\| + \|{}_0^c D_{t_{n-\sigma}}^\alpha R_h u - {}_0^c D_{t_{n-\sigma}}^\alpha u\| + m_2 \|\Delta u^{n,\sigma} - \Delta u^{n-\sigma}\|\\ &+ \left|M\left(\int_\Omega U_h^{n,\sigma}\, dx\right) - M\left(\int_\Omega u^{n-\sigma}\, dx\right)\right| \|\Delta u^{n,\sigma}\|\Big) \|\eta^{n,\sigma}\|.\end{aligned} \tag{4.26}$$

From (4.17), Theorem 4.7, Lipschitz continuity of function M, and triangle inequality, we get

$$\begin{aligned}D_N^\alpha \|\eta^{n-\sigma}\|^2 \le C\big[\|\eta^{n,\sigma}\|^2 + \big(&\|D_N^\alpha R_h u^{n-\sigma} - {}_0^c D_{t_{n-\sigma}}^\alpha R_h u\| + \|\Delta u^{n,\sigma} - \Delta u^{n-\sigma}\|\\ &+ h^{m+1} + \|u^{n,\sigma} - u^{n-\sigma}\|\big)\|\eta^{n,\sigma}\|\big].\end{aligned} \tag{4.27}$$

By using Poincaré inequality, we get

$$\begin{aligned}D_N^\alpha \|\eta^{n-\sigma}\|^2 \le C\big[\|\eta^{n,\sigma}\|^2 + \big(&\|\nabla(D_N^\alpha R_h u^{n-\sigma} - {}_0^c D_{t_{n-\sigma}}^\alpha R_h u)\| + \|\Delta u^{n,\sigma} - \Delta u^{n-\sigma}\|\\ &+ h^{m+1} + \|u^{n,\sigma} - u^{n-\sigma}\|\big)\|\eta^{n,\sigma}\|\big].\end{aligned} \tag{4.28}$$

Now, we use Lemma 4.3 in (4.28), we get

$$\begin{aligned}\|\eta^n\| \le 2\,C E_\alpha\left(2\Lambda\pi_A\, t_n^\alpha\right)\Bigg[\|\eta^0\| + \max_{1\le k\le n}\sum_{j=1}^{k} Q_{k-j}^{(k)}\Big(&\|\nabla(D_N^\alpha u^{j-\sigma} - {}_0^c D_{t_{j-\sigma}}^\alpha u)\|\\ &+ \|\Delta u^{j,\sigma} - \Delta u^{j-\sigma}\| + h^{m+1} + \|u^{j,\sigma} - u^{j-\sigma}\|\Big)\Bigg].\end{aligned} \tag{4.29}$$

From Lemma 4.6 and Lemma 4.5, we get

$$\begin{aligned}&\|\nabla(D_N^\alpha u^{j-\sigma} - {}_0^c D_{t_{j-\sigma}}^\alpha u)\| + \|\Delta u^{j,\sigma} - \Delta u^{j-\sigma}\| + \|u^{j,\sigma} - u^{j-\sigma}\|\\ &\le \begin{cases} C t_{j-\sigma}^{-\alpha}\left(N^{-\min\{3-\alpha,\, r\alpha\}} + N^{-\min\{2,\, r\alpha\}}\right), & \text{if } \sigma = \frac{\alpha}{2},\\ C t_j^{-\alpha}\, N^{-\min\{2-\alpha,\, r\alpha\}}, & \text{if } \sigma = 0.\end{cases}\end{aligned} \tag{4.30}$$

If $l_N = \frac{1}{\ln N}$ then we get following inequalities

$$t_{j-\sigma}^{-\alpha} \le \begin{cases} (j/2)^{-r\alpha} N^{r\alpha} \le (2N)^{r\alpha} j^{r(l_N-\alpha)}, & \text{if } \sigma = \frac{\alpha}{2},\\ j^{-r\alpha} N^{r\alpha} \le N^{r\alpha} j^{r(l_N-\alpha)}, & \text{if } \sigma = 0.\end{cases} \tag{4.31}$$

Setting $\gamma = l_N$ in Lemma 4.2 then we get

$$\sum_{j=1}^{k} Q_{k-j}^{(k)}\, j^{r(l_N-\alpha)} \le \frac{\pi_A\, \Gamma(1 + l_N - \alpha)}{\Gamma(1 + l_N)} T^\alpha\, N^{r(l_N-\alpha)}. \tag{4.32}$$

Now, we use (4.32), (4.31), and (4.30) in (4.29), and then we get

$$\|\eta^n\| \leq \begin{cases} C\left[\|\eta^0\| + (2N)^{r\alpha}\left(\frac{11\,\Gamma(1+l_N-\alpha)}{4\Gamma(1+l_N)}T^\alpha\ N^{r(l_N-\alpha)}(N^{-\min\{3-\alpha,\,r\alpha\}}\right.\right. \\ \left.\left.+N^{-\min\{2,\,r\alpha\}}\right)\right) + \max\limits_{1\leq k\leq n}\sum\limits_{j=1}^{k} Q_{k-j}^{(k)}h^{m+1}\right] & \text{if } \sigma=\frac{\alpha}{2}, \\ C\left[\|\eta^0\| + N^{r\alpha}\left(\frac{\Gamma(1+l_N-\alpha)}{\Gamma(1+l_N)}T^\alpha\ N^{r(l_N-\alpha)}N^{-\min\{2-\alpha,\,r\alpha\}}\right)\right. \\ \left.+\max\limits_{1\leq k\leq n}\sum\limits_{j=1}^{k} Q_{k-j}^{(k)}h^{m+1}\right] & \text{if } \sigma=0. \end{cases} \tag{4.33}$$

Taking $\gamma=\alpha$ in Lemma 4.2 then we get

$$\sum_{j=1}^{k} Q_{k-j}^{(k)} \ \leq\ \frac{\pi_A}{\Gamma(1+\alpha)}T^\alpha. \tag{4.34}$$

If we choose $U_h^0 = R_h u^0$ then $\|\eta^0\|=0$, and using (4.34) in (4.33), we get

$$\|\eta^n\| \leq \begin{cases} C\left[(2N)^{r\alpha}\left(\frac{11\,\Gamma(1+l_N-\alpha)}{4\Gamma(1+l_N)}T^\alpha\ N^{r(l_N-\alpha)}(N^{-\min\{3-\alpha,\,r\alpha\}}\right.\right. \\ \left.\left.+N^{-\min\{2,\,r\alpha\}}\right)\right) + \frac{11}{4\,\Gamma(1+\alpha)}T^\alpha h^{m+1}\right], & \text{if } \sigma=\frac{\alpha}{2}, \\ C\left[N^{r\alpha}\left(\frac{\Gamma(1+l_N-\alpha)}{\Gamma(1+l_N)}T^\alpha\ N^{r(l_N-\alpha)}N^{-\min\{2-\alpha,\,r\alpha\}}\right)\right. \\ \left.+\frac{1}{\Gamma(1+\alpha)}T^\alpha h^{m+1}\right], & \text{if } \sigma=0. \end{cases} \tag{4.35}$$

Now, we can utilize Theorem 4.7 and the triangle inequality to get the first desired result (4.24b). From equation (4.13), we can rewrite equation (4.25) as follows:

$$\begin{aligned} \left(D_N^\alpha \eta^{n-\sigma},\psi_h\right) - M\left(\int_\Omega U_h^{n,\sigma}\,dx\right)\left(\Delta_h\eta^{n,\sigma},\psi_h\right) \ &=\ \left(D_N^\alpha R_h u^{n-\sigma} - {}_0^c D_{t_{n-\sigma}}^\alpha u,\psi_h\right) \\ &\quad - M\left(\int_\Omega u^{n-\sigma}\,dx\right)\left(\Delta u^{n,\sigma}-\Delta u^{n-\sigma},\psi_h\right) \\ &\quad - \left(M\left(\int_\Omega U_h^{n,\sigma}\,dx\right) - M\left(\int_\Omega u^{n-\sigma}\,dx\right)\right)\left(\Delta u^{n,\sigma},\psi_h\right). \end{aligned} \tag{4.36}$$

Choosing $\psi_h = -\Delta_h\eta^{n,\sigma}$ in (4.36) then use Cauchy-Schwarz inequality, triangle inequality, Lemma 4.1 and assumption $H2$ together with (4.19) and (4.20) to get

$$\begin{aligned} \frac{1}{2}D_N^\alpha\|\nabla\eta^{n-\sigma}\|^2 + m_1\|\Delta_h\eta^{n,\sigma}\|^2 &\leq \|\nabla(D_N^\alpha R_h u^{n-\sigma} - {}_0^c D_{t_{n-\sigma}}^\alpha R_h u)\|\|\nabla\eta^{n,\sigma}\| \\ &\quad + \|\nabla({}_0^c D_{t_{n-\sigma}}^\alpha R_h u - P_h({}_0^c D_{t_{n-\sigma}}^\alpha u))\|\|\nabla\eta^{n,\sigma}\| \\ &\quad + m_2\|\nabla P_h(\Delta u^{n,\sigma}-\Delta u^{n-\sigma})\|\|\nabla\eta^{n,\sigma}\| \\ &\quad + \left|M\left(\int_\Omega U_h^{n,\sigma}\,dx\right) - M\left(\int_\Omega u^{n-\sigma}\,dx\right)\right|\|\nabla P_h(\Delta u^{n,\sigma})\|\|\nabla\eta^{n,\sigma}\| \\ &\leq C\Big(\left(\|\nabla(D_N^\alpha R_h u^{n-\sigma} - {}_0^c D_{t_{n-\sigma}}^\alpha R_h u)\| + \|\nabla({}_0^c D_{t_{n-\sigma}}^\alpha R_h u - {}_0^c D_{t_{n-\sigma}}^\alpha u)\|\right. \\ &\quad \left. + m_2\|\nabla(\Delta u^{n,\sigma}-\Delta u^{n-\sigma})\|\right)\|\nabla\eta^{n,\sigma}\| \end{aligned}$$

$$+\left|M\Big(\int_\Omega U_h^{n,\sigma}\,dx\Big)-M\Big(\int_\Omega u^{n-\sigma}\,dx\Big)\right|\|\nabla(\Delta u^{n,\sigma})\|\|\nabla\eta^{n,\sigma}\|\Big). \tag{4.37}$$

From (4.17), Theorem 4.7, Lipschitz continuity of function M, Poincaré inequality and triangle inequality, we get

$$\begin{aligned} D_N^\alpha\|\nabla\eta^{n-\sigma}\|^2 \le C\big(&\|\nabla\eta^{n,\sigma}\|^2+\big(\|\nabla(D_N^\alpha R_h u^{n-\sigma}-{}_0^cD_{t_{n-\sigma}}^\alpha R_h u)\|\\ &+\|\nabla(\Delta u^{n,\sigma}-\Delta u^{n-\sigma})\|h^m+\|\nabla(u^{n,\sigma}-u^{n-\sigma})\|\big)\|\nabla\eta^{n,\sigma}\|\big). \end{aligned} \tag{4.38}$$

Now, we use Lemma 4.3 in (4.38) and follow a similar argument as above, one can get the error estimate in H_0^1-norm. This completes the proof. □

5. Numerical Experiments

In this numerical experiments section, we conduct three numerical experiments on different domains. All simulations are performed with MATLAB R2024a on a computer system having Intel Xeon processor running at 3.90 GHz, 256 GB of RAM. To solve all examples using the scheme (4.2), we set $T = 0.5$. For the $L1$ scheme, we choose $r = \frac{2-\alpha}{2}$, and for the $L2\text{-}1_\sigma$ scheme, we set $r = \frac{3-\alpha}{3}$ to achieve the desired convergence rate. For Newton's iterations, we select the initial guess u^g as the solution to the Poisson equation under the homogeneous Dirichlet boundary condition and set the tolerance to 10^{-15}. To get errors and rate of convergence in the spatial direction, we run the test for $\alpha = 0.5$ while $\alpha = 0.4$, 0.6, and 0.8 are used to calculate temporal errors and convergence rates. We compute relative spatial errors E_1 and E_2 at the final time level through $E_1 = \frac{\|u^N-U_h^N\|}{\|u^N\|}$ and $E_2 = \frac{\|\nabla u^N-\nabla U_h^N\|}{\|\nabla u^N\|}$. Furthermore, the maximum relative temporal error E_3 is calculated using $E_3 = \dfrac{\max\limits_{1\le n\le N}\|u^n-U_h^n\|}{\max\limits_{1\le n\le N}\|u^n\|}$.

We have achieved the theoretical convergence orders $O\big(h^{m+1}+N^{-\min\{2-\alpha,\,r\alpha\}}\big)$ and $O\big(h^{m+1}+N^{-\min\{2,\,r\alpha\}}\big)$ of the fully-discrete scheme (4.2) for $L1$ and $L2\text{-}1_\sigma$ methods, respectively in the $L^2(\Omega)$ norm. Similarly, the established convergence orders in the $H_0^1(\Omega)$ norm are $O\big(h^m+N^{-\min\{2-\alpha,\,r\alpha\}}\big)$ and $O\big(h^m+N^{-\min\{2,\,r\alpha\}}\big)$ for the $L1$ and $L2\text{-}1_\sigma$ methods, respectively. We therefore calculate $L^2(\Omega)$ relative errors (E_1), $H_0^1(\Omega)$ relative errors (E_2) by using the relations $N = \left\lfloor \frac{1}{h^{\frac{m+1}{2-\alpha}}} \right\rfloor$, $\left\lfloor \frac{1}{h^{\frac{m}{2-\alpha}}} \right\rfloor$ (for $L1$ scheme) and $N = \left\lfloor \frac{1}{h^{\frac{m+1}{2}}} \right\rfloor$, $\left\lfloor \frac{1}{h^{\frac{m}{2}}} \right\rfloor$ (for $L2\text{-}1_\sigma$ scheme). Further, we set $h^{-1} = \left\lfloor N^{\frac{2-\alpha}{m+1}} \right\rfloor$ (h^{-1} is a number of cells per coordinate direction) for $L1$ method based scheme and $h^{-1} = \left\lfloor N^{\frac{2}{m+1}} \right\rfloor$ for the $L2\text{-}1_\sigma$ method based scheme to compute maximum relative errors (E_3) for various α-values.

Example 5.1. Consider the time-fractional nonlocal diffusion Equation (1.1) with the nonlocal term $M\big(\int_\Omega u\,dx\big) = 3+\int_\Omega u\,dx$ on unit square Ω. The weight function associated with this domain is given by $w = (1-x)(1-y)xy$. The source function f is chosen in such a manner that the exact solution is $u = (t^3+t^\alpha)\cos(\pi x)w$. We solve the considered example using fully-discrete scheme (4.2) for various α-values. For comparison, we also solve Example 5.1 using $L1$ and $L2\text{-}1_\sigma$ methods with the standard FEM. Tables 1 and 2 provide results of a comparison between these two methods. The weighted b-spline method exhibits better accuracy compared to the standard FEM, as evidenced by the errors and rates of convergence presented in Tables 1 and 2 corresponding to different degrees of freedom (DOF).

Furthermore, the numerical outcomes obtained using the proposed $L1$ and $L2\text{-}1_\sigma$ methods under scheme (4.2) are presented in Tables 3–5. In Table 3, we report maximum relative errors (E_3) and corresponding convergence rates. Tables 4 and 5 show $L^2(\Omega)$ relative errors (E_1) and $H_0^1(\Omega)$ relative errors (E_2), respectively with corresponding rates of convergence for weighted b-splines of degree $m = 1,\ 2,\ 3$. Finally, we display the plot of the approximate solution and its domain Ω in Figure 2.

Example 5.2. Consider the time-fractional nonlocal diffusion equation (1.1) with the nonlocal term

$$M\big(\int_\Omega u\,dx\big) = 3+\int_\Omega u\,dx,$$

TABLE 1. Relative errors and rates (dominated by spatial error) for the $L1$ scheme for the Example 5.1.

Error	DOF	Weighted b-spline method error	Rate	Standard FEM error	Rate
E_1	81	0.8760E-2		0.1444E-0	
	289	0.2262E-2	1.9533	0.3288E-1	2.1349
	1089	0.5694E-3	1.9899	0.7773E-2	2.0808
	4225	0.1425E-3	1.9980	0.1886E-2	2.0430
E_2	81	0.2823E-1		1.8479E-0	
	289	0.1399E-1	1.0127	0.8549E-0	1.1119
	1089	0.6942E-2	1.0109	0.4129E-0	1.0497
	4225	0.3461E-2	1.0040	0.2031E-0	1.0236

TABLE 2. Relative errors and rates (dominated by spatial error) for the $L2\text{-}1_\sigma$ scheme for the Example 5.1.

Error	DOF	Weighted b-spline method error	Rate	Standard FEM error	Rate
E_1	81	0.1804E-1		0.1057E-0	
	289	0.5937E-2	1.6033	0.2787E-1	1.9231
	1089	0.1670E-2	1.8295	0.7104E-2	1.9720
	4225	0.4399E-3	1.9250	0.1789E-2	1.9892
E_2	81	0.4389E-1		0.2091E-0	
	289	0.2186E-1	1.0055	0.1040E-0	1.0068
	1089	0.1080E-2	1.0171	0.5195E-1	1.0023
	4225	0.5374E-2	1.0070	0.2596E-1	1.0006

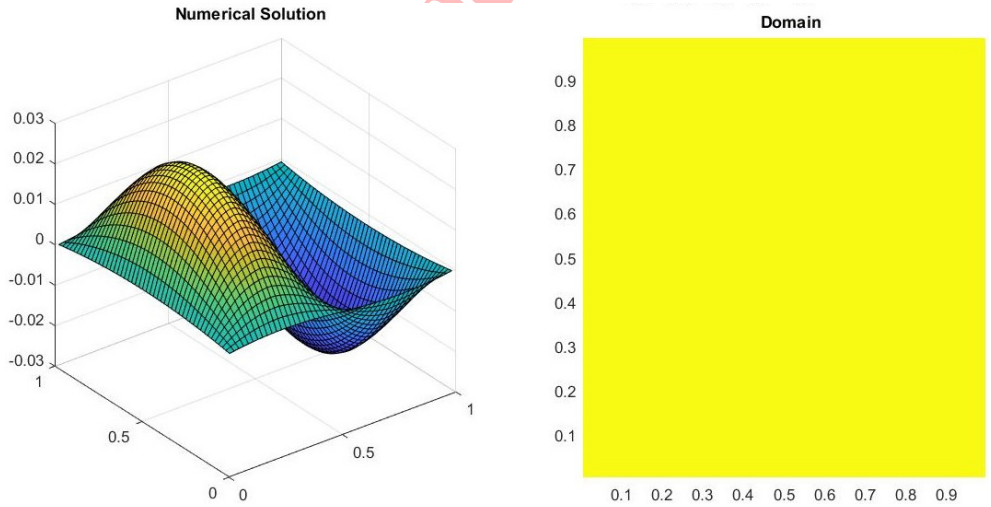

FIGURE 2. Plot of the numerical solution and its domain at $T = 0.5$ and $\alpha = 0.5$ for Example 5.1.

on shovel type domain Ω. The weight function associated with this domain is given by $w = 1 - X^2 - \left(\frac{Y}{2} + X^2 - 1\right)^2$ for $X = 2x - 1$ and $Y = 5y - 1$. The source function f is chosen in such a manner that the exact

TABLE 3. Maximum relative errors (E_3) and rates (dominated by temporal error) for Example 5.1.

	N	$L1$ scheme	Rate	N	$L2$-1_σ scheme	Rate
$\alpha = 0.4$	16	0.7371E-2		16	0.6604E-2	
	81	0.5665E-3	1.5820	32	0.2007E-2	1.7176
	256	0.8752E-4	1.6230	64	0.5485E-3	1.8719
	625	0.2086E-4	1.6061	128	0.1429E-3	1.9403
$\alpha = 0.6$	16	0.1469E-1		16	0.5395E-1	
	81	0.1310E-2	1.4902	32	0.1446E-2	1.7464
	256	0.2517E-3	1.4334	64	0.1310E-2	1.8989
	625	0.7165E-4	1.4079	128	0.9440E-4	1.9571
$\alpha = 0.8$	16	0.2049E-1		16	0.4473E-2	
	81	0.3032E-2	1.1782	32	0.1144E-2	1.9671
	256	0.7659E-3	1.1956	64	0.2884E-3	1.9878
	625	0.2626E-3	1.1989	128	0.7236E-4	1.9950

TABLE 4. Relative errors (E_1) and rates (dominated by spatial error) for Example 5.1.

Degree	DOF	$L1$ Scheme	Rate	$L2$-1_σ scheme	Rate
$m = 1$	81	0.8760E-2		0.1804E-1	
	289	0.2262E-2	1.9533	0.5937E-2	1.6033
	1089	0.5694E-3	1.9899	0.1670E-2	1.8295
	4225	0.1425E-3	1.9980	0.4399E-3	1.9250
$m = 2$	100	0.5927E-3		0.2802E-2	
	324	0.7233E-4	3.0346	0.3740E-3	2.9057
	1156	0.8988E-5	3.0085	0.4839E-4	2.9502
	4336	0.1122E-5	3.0020	0.6114E-5	2.9843
$m = 3$	121	0.2441E-4		0.3662E-3	
	361	0.1398E-5	4.1269	0.2390E-4	3.9378
	1225	0.8543E-7	4.0327	0.1508E-5	3.9857
	4489	0.5309E-8	4.0082	0.9449E-7	3.9968

TABLE 5. Relative errors (E_2) and rates (dominated by spatial error) for Example 5.1.

Degree	DOF	$L1$ scheme	Rate	$L2$-1_σ scheme	Rate
$m = 1$	81	0.2823E-1		0.4389E-1	
	289	0.1399E-1	1.0127	0.2186E-1	1.0055
	1089	0.6942E-2	1.0109	0.1080E-2	1.0171
	4225	0.3461E-2	1.0040	0.5374E-2	1.0070
$m = 2$	100	0.4250E-2		0.4946E-2	
	324	0.1048E-2	2.0186	0.1082E-2	2.1913
	1156	0.2613E-3	2.0046	0.2583E-3	2.0674
	4336	0.6529E-4	2.0011	0.6372E-4	2.0195
$m = 3$	121	0.1658E-3		0.3997E-3	
	361	0.1967E-4	3.0751	0.3060E-4	3.7073
	1225	0.2426E-5	3.0193	0.2800E-5	3.4500
	4489	0.3023E-6	3.0047	0.3087E-6	3.1809

TABLE 6. Maximum relative errors (E_3) and rates (dominated by temporal error) for the Example 5.2.

	N	$L1$ scheme	Rate	N	$L2\text{-}1_\sigma$ scheme	Rate
$\alpha = 0.4$	16	0.1308E-1		16	0.8170E-2	
	81	0.1020E-2	1.5730	32	0.2379E-2	1.7797
	256	0.1634E-3	1.5916	64	0.6389E-3	1.8969
	625	0.3900E-4	1.6055	128	0.1652E-3	1.9513
$\alpha = 0.6$	16	0.2789E-1		16	0.7067E-2	
	81	0.2590E-2	1.4654	32	0.1861E-2	1.9248
	256	0.4834E-3	1.4586	64	0.4754E-3	1.9688
	625	0.1376E-3	1.4072	128	0.1200E-3	1.9862
$\alpha = 0.8$	16	0.3976E-1		16	0.6248E-2	
	81	0.6010E-2	1.1650	32	0.1591E-2	1.9727
	256	0.1521E-2	1.1941	64	0.4005E-3	1.9908
	625	0.5213E-3	1.1995	128	0.1003E-3	1.9966

TABLE 7. Relative errors (E_1) and rates (dominated by spatial error) for the Example 5.2.

Degree	DOF	$L1$ scheme	Rate	$L2\text{-}1_\sigma$ scheme	Rate
m=1	81	0.1636E-1		0.2478E-1	
	289	0.4286E-2	1.9324	0.7580E-2	1.7091
	1089	0.1085E-2	1.9818	0.2072E-2	1.8712
	4225	0.2721E-3	1.9957	0.5388E-3	1.9430
m=2	100	0.1048E-2		0.2867E-2	
	324	0.1267E-3	3.0484	0.3832E-3	2.9034
	1156	0.1566E-4	3.0162	0.4963E-4	2.9488
	4336	0.1951E-5	3.0045	0.6278E-5	2.9828
m=3	121	0.1084E-3		0.3789E-3	
	361	0.6836E-5	3.9875	0.2468E-4	3.9400
	1225	0.4276E-6	3.9987	0.1557E-5	3.9863
	4489	0.2673E-7	3.9998	0.9758E-6	3.9964

solution is $u = (t^3 + t^\alpha)w^2$. The numerical outcomes obtained through proposed $L1$ and $L2\text{-}1_\sigma$ methods based scheme (4.2) are exhibited in Tables 6–8. In Table 6, we report maximum relative errors (E_3) and corresponding convergence rates. Tables 7 and 8 show $L^2(\Omega)$ relative errors (E_1) and $H_0^1(\Omega)$ relative errors (E_2), respectively with corresponding rates of convergence for weighted b-splines of degree $m = 1,\ 2,\ 3$. Finally, we display the plot of the approximate solution and its domain Ω in Figure 3.

Example 5.3. Consider the time-fractional nonlocal diffusion equation (1.1) with the nonlocal term $M\big(\int_\Omega u\ dx\big) = 3 + \cos\big(\int_\Omega u\ dx\big)$ on domain Ω which is bounded by an ellipse $E = \{(x,y) := r_1^{'}(x,y) \geq 0\}$, $r_1^{'} = \left(1 - \left(\frac{x-\frac{1}{2}}{0.49}\right)^2 - \left(\frac{y-\frac{1}{2}}{0.25}\right)^2\right)$, and a circle $C = \{(x,y) := r_2^{'}(x,y) \geq 0\}$, $r_2^{'} = \left(x-\frac{1}{2}\right)^2 + \left(y-\frac{1}{2}\right)^2 - \left(\frac{1}{8}\right)^2$. The weight function associated with this domain is given by $w = r_1^{'} r_2^{'}$. The source function f is chosen in such a manner that the exact solution is $u = (t^3 + t^\alpha)w \sin w$. The numerical outcomes obtained through proposed $L1$ and $L2\text{-}1_\sigma$ methods based scheme (4.2) are exhibited in Tables 9–11. In Table 9, we report maximum relative errors (E_3) and corresponding convergence rates. Tables 10 and 11 show $L^2(\Omega)$ relative errors (E_1) and $H_0^1(\Omega)$ relative errors (E_2), respectively with corresponding rates of convergence for weighted b-splines of degree $m = 1,\ 2,\ 3$. Finally, we display the plot of the approximate solution and its domain Ω in Figure 4.

TABLE 8. Relative errors (E_2) and rates (dominated by spatial error) for the Example 5.2.

Degree	DOF	$L1$ scheme	Rate	$L2\text{-}1_\sigma$ scheme	Rate
m=1	81	0.7704E-1		0.7999E-1	
	289	0.3850E-1	1.0005	0.3919E-1	1.0294
	1089	0.1917E-1	1.0057	0.1918E-1	1.0228
	4225	0.9567E-2	1.0030	0.9583E-2	1.0090
m=2	100	0.6116E-2		0.6697E-2	
	324	0.1509E-2	2.0184	0.1553E-2	2.1080
	1156	0.3755E-3	2.0072	0.3785E-3	2.0369
	4336	0.9374E-4	2.0021	0.9393E-4	2.0106
m=3	121	0.6611E-3		0.7552E-3	
	361	0.8286E-4	2.9962	0.8621E-4	3.1308
	1225	0.1035E-4	3.0010	0.1045E-4	3.0432
	4489	0.1293E-5	3.0005	0.1296E-5	3.0117

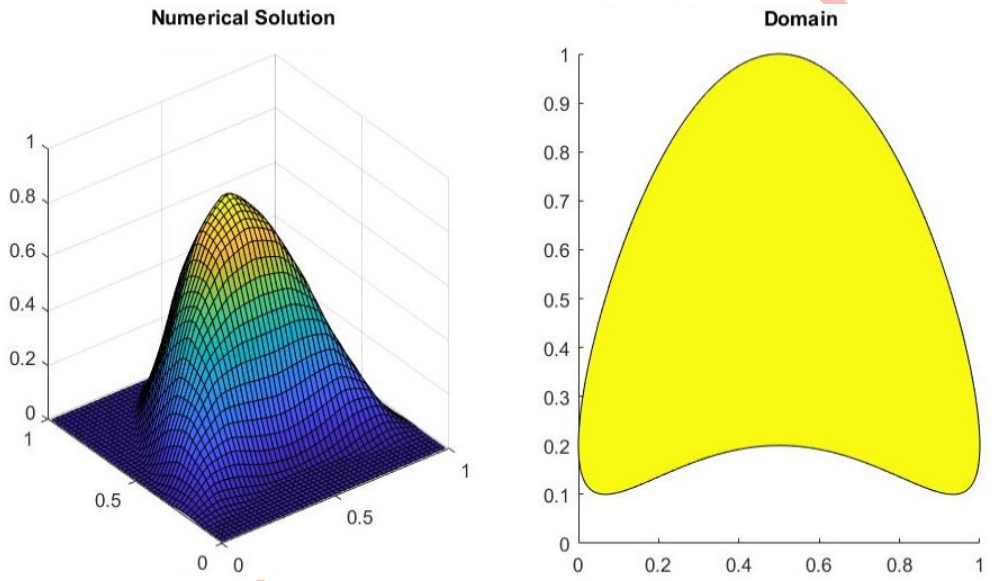

FIGURE 3. Plot of the numerical solution and its domain at $T = 0.5$ and $\alpha = 0.5$ for Example 5.2.

6. CONCLUSION

In this paper, we solved a time-fractional diffusion equation with a nonlocal diffusion term by proposing a fully-discrete scheme in a unified way. The scheme resulted in $O\big(N^{-\min\{2-\alpha,\, r\alpha\}}\big)$ and $O\big(N^{-\min\{2,\, r\alpha\}}\big)$ convergence in time for $L1$ and $L2\text{-}1_\sigma$ methods, respectively in both $L^2(\Omega)$ and $H_0^1(\Omega)$ norms. The scheme also generated $O\big(h^{m+1}\big)$ and $O\big(h^m\big)$ convergence in space in $L^2(\Omega)$ and $H_0^1(\Omega)$ norms, respectively. A comparison of solutions obtained from weighted b-spline and standard FEM clearly exhibited more accurate results associated with the proposed weighted b-spline method.

ACKNOWLEDGMENT

The authors express their gratitude to the anonymous reviewers for their insightful suggestions and comments. The first author would like to express gratitude to the Council of Scientific and Industrial Research

TABLE 9. Maximum relative errors (E_3) and rates (dominated by temporal error) for the Example 5.3.

	N	$L1$ scheme	Rate	N	$L2\text{-}1_\sigma$ scheme	Rate
$\alpha = 0.4$	16	0.6364E-1		16	0.2500E-1	
	81	0.5924E-2	1.4639	32	0.6683E-2	1.9036
	256	0.9502E-3	1.5905	64	0.1709E-2	1.9676
	625	0.2284E-4	1.5973	128	0.4302E-3	1.9898
$\alpha = 0.6$	16	0.9459E-1		16	0.2474E-2	
	81	0.1346E-1	1.2019	32	0.6568E-2	1.9134
	256	0.2776E-2	1.3725	64	0.1673E-2	1.9727
	625	0.7957E-3	1.3998	128	0.4205E-3	1.9925
$\alpha = 0.8$	16	0.1492E-0		16	0.2459E-1	
	81	0.3456E-1	0.9019	32	0.6515E-2	1.9162
	256	0.8755E-2	1.1932	64	0.1658E-2	1.9741
	625	0.2986E-2	1.2049	128	0.4165E-3	1.9932

TABLE 10. Relative errors (E_1) and rates (dominated by spatial error) for the Example 5.3.

Degree	DOF	$L1$ scheme	Rate	$L2\text{-}1_\sigma$ scheme	Rate
m=1	81	0.7011E-1		0.7671E-1	
	289	0.2371E-1	1.5640	0.2583E-1	1.5703
	1089	0.6290E-2	1.9145	0.6820E-2	1.9213
	4225	0.1602E-2	1.9735	0.1683E-2	2.0187
m=2	100	0.1455E-1		0.1460E-1	
	324	0.1712E-2	3.0873	0.1741E-2	3.0680
	1156	0.2112E-3	3.0187	0.2160E-3	3.0111
	4336	0.2622E-4	3.0098	0.2688E-4	3.0063
m=3	121	0.1817E-2		0.1847E-2	
	361	0.1390E-3	3.7088	0.1409E-3	3.7121
	1225	0.8822E-5	3.9779	0.8948E-5	3.9772
	4489	0.5516E-6	3.9993	0.5596E-6	3.9991

TABLE 11. Relative errors (E_2) and rates (dominated by spatial error) for the Example 5.3.

Degree	DOF	$L1$ scheme	Rate	$L2\text{-}1_\sigma$ scheme	Rate
m=1	81	0.1618E-0		0.2305E-0	
	289	0.9343E-1	0.7924	0.1271E-0	0.8585
	1089	0.4644E-1	1.0085	0.6372E-1	0.9966
	4225	0.2305E-1	1.0105	0.3166E-1	1.0091
m=2	100	0.3521E-1		0.3762E-1	
	324	0.8772E-2	2.0052	0.1000E-1	1.9111
	1156	0.2185E-2	2.0051	0.2590E-2	1.9488
	4336	0.5445E-3	2.0047	0.6589E-3	1.9753
m=3	121	0.5060E-2		0.7036E-2	
	361	0.7365E-3	2.7804	0.9889E-3	2.8307
	1225	0.9259E-4	2.9917	0.1250E-3	2.9837
	4489	0.1155E-4	3.0024	0.1564E-4	2.9984

for providing the Ph.D. scholarship. This work is part of the author's doctoral thesis under the supervision of Dr. Sudhakar Chaudhary.

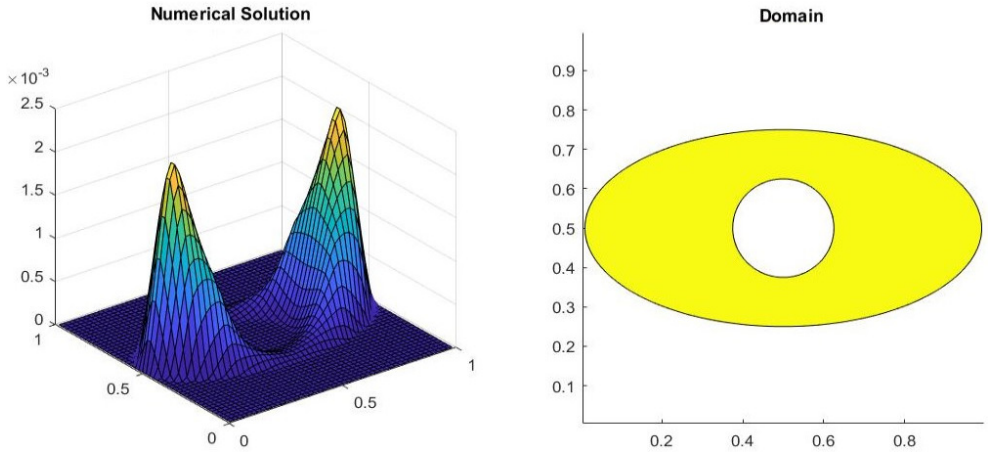

FIGURE 4. Plot of the numerical solution and its domain at $T = 0.5$ and $\alpha = 0.5$ for Example 5.3.

REFERENCES

[1] A. Alikhanov, *A new difference scheme for the time-fractional diffusion equation*, J. Comput. Phys., *280* (2015), 424–438.

[2] H. Azin, A. Habibirad, and O. Baghani, *Legendre-finite difference method for solving fractional nonlinear Sobolev equation with Caputo derivative*, J. Comput. Sci., *74* (2023), 102177.

[3] S. Chaudhary and J. P. Mandaliya, *Mesh-free Galerkin approximation for parabolic nonlocal problem using web-splines*, Comput. Math. Appl., *128* (2022), 180–187.

[4] S. Chaudhary, V. Srivastava, V. V. K. Srinivas Kumar, and B. Srinivasan, *Finite element approximation of nonlocal parabolic problem*, Numer. Methods Partial Differ. Eq., *33* (2017), 786–813.

[5] S. Chaudhary and P. J. Kundaliya, *L1 scheme on graded mesh for subdiffusion equation with nonlocal diffusion term*, Math. Comput. Simul., *195* (2022), 119–137.

[6] H. Chen and M. Stynes, *Blow-up of error estimates in time-fractional initial-boundary value problems*, IMA J. Numer. Anal., *41*(2) (2021), 974–997.

[7] H. Chen, Y. Wang, and H. Fu, *α-robust H^1-norm error estimate of nonuniform Alikhanov scheme for fractional sub-diffusion equation*, Appl. Math. Lett., *125* (2022), 107771.

[8] M. Chipot and M. Siegwart, *On the asymptotic behavior of some nonlocal mixed boundary value problems*, Nonlinear Anal. Real World Appl., *1* (2003), 431–450.

[9] K. Diethelm, *The Analysis of Fractional Differential Equations: An Application-Oriented Using Differential Operators of Caputo Type*, Lecture Notes in Mathematics, Springer, 2010.

[10] T. Gudi, *Finite element method for a nonlocal problem of Kirchhoff type*, SIAM J. Numer. Anal., *50*(2) (2012), 657–668.

[11] A. R. Hadhoud, P. Agarwal, and A. A. Rageh, *Numerical treatments of the nonlinear coupled time-fractional Schrödinger equations*, Math. Methods Appl. Sci., *45*(11) (2022), 7119–7143.

[12] K. Höllig, U. Reif, and J. Wipper, *Weighted extended B-spline approximation of Dirichlet problems*, SIAM J. Numer. Anal., *39*(2) (2001), 442–462.

[13] K. Höllig, *Finite Element Methods with B-Splines*, Philadelphia, SIAM., 2003.

[14] K. Höllig and J. Hörner, *Programming finite element methods with weighted B-splines*, Comput. Math. Appl., *70*(7) (2015), 1441–1456.

[15] C. Huang and M. Stynes, *α-robust error analysis of a mixed finite element method for a time-fractional biharmonic equation*, Numer. Algorithms, *87*(4) (2021), 1749–1766.

[16] C. Huang and M. Stynes, *A sharp α-robust $L^\infty(H^1)$ error bound for a time-fractional Allen-Cahn problem discretised by the Alikhanov L2-1$_\sigma$ scheme and a standard FEM*, J. Sci. Comput., *91*(2) (2022),

43.
[17] C. Huang and M. Stynes, *Optimal spatial H^1-norm analysis of a finite element method for a time-fractional diffusion equation*, J. Comput. Appl. Math., *367* (2020), 112435.
[18] B. Jin, B. Li, and Z. Zhou, *Numerical analysis of nonlinear subdiffusion equations*, SIAM J. Numer. Anal., *56*(1) (2018), 1–23.
[19] P. J. Kundaliya, *α-Robust Error Analysis of L2-1$_\sigma$ Scheme on Graded Mesh for Time-fractional Nonlocal Diffusion Equation*, J. Comput. Nonlinear Dynam., *19*(5) (2023), 051004.
[20] G. T. Lubo and G. F. Duressa, *Linear b-spline finite element method for solving delay reaction diffusion equation*, Comput. Methods Differ. Equ., *11*(1) (2023), 161–174.
[21] Y. F. Luchko, M. Rivero, J. J. Trujillo, and M. P. Velasco, *Fractional models, nonlocality, and complex systems*, Comput. Math. Appl., *59*(3) (2010), 1048–1056.
[22] J. Manimaran, L. Shangerganesh, A. Debbouche, and V. Antonov, *Numerical solutions for time-fractional cancer invasion system with nonlocal diffusion*, Front. Phys., *7* (2019), 93.
[23] F. Mirzaee and N. Samadyar, *Implicit meshless method to solve 2D fractional stochastic Tricomi-type equation defined on irregular domain occurring in fractal transonic flow*, Numer. Methods Partial Differ. Eq., *37* (2021), 1781–1799.
[24] S. Patra and V. V. K. Srinivas Kumar, *Finite element approximation using web-splines for the heat equation*, Numer. Funct. Anal. Optim., *39*(13) (2018), 1423–1439.
[25] S. Rida, A. El-Sayed, and A. Arafa, *Effect of bacterial memory dependent growth by using fractional derivatives reaction-diffusion chemotactic model*, J. Stat. Phys., *140*(4) (2010), 797–811.
[26] V. L. Rvachev and T. I. Sheiko, *R-functions in boundary value problems in mechanics*, Appl. Mech. Rev., *48* (1995), 151–188.
[27] A. Singh, S. Kumar, and J. Vigo-Aguiar, *A fully discrete scheme based on cubic splines and its analysis for time-fractional reaction–diffusion equations exhibiting weak initial singularity*, J. Comput. Appl. Math., *434* (2023), 115338.
[28] D. Singh, R. K. Pandey, and S. Kumari, *A fourth order accurate numerical method for non-linear time fractional reaction–diffusion equation on a bounded domain*, Physica D., *130* (2024), 107769.
[29] R. Singh, A. Singh, S. Kumar, and J. Vigo-Aguiar, *A novel high-order approximation method for higher-dimensional time-fractional reaction-diffusion problems with weak initial singularity*, Comput. Methods Differ. Equ., *13*(3) (2025), 980–994.
[30] M. Stynes, E. O'Riordan, and J. Gracia, *Error analysis of a finite difference method on graded meshes for a time-fractional diffusion equation*, SIAM J. Numer. Anal., *55* (2017), 1057–1079.
[31] V. Thomée, *Galerkin Finite Element Methods for Parabolic Problems*, Second revised and expanded ed., Springer, Berlin, 2006.
[32] J. R. L. Webb, *Weakly singular Gronwall inequalities and applications to fractional differential equations*, J. Math. Anal. Appl., *471*(1–2) (2019), 692–711.
[33] W. K. Zahra, M. M. Hikal, and D. Baleanu, *Numerical simulation for time-fractional nonlinear reaction–diffusion system on a uniform and nonuniform time stepping*, Math. Methods Appl. Sci., *44*(7) (2021), 5340–5364.